Effects of Frequency and Temperature on Partial Discharge Characterization of Stator Windings

Emre Kantar, Espen Eberg, and Sverre Hvidsten
Department of Electric Power Technology, SINTEF Energy Research, Trondheim, Norway

***Abstract*—This paper presents results from laboratory measurements of partial discharge (PD) activity in stator bars taken from a 13-kV/95-MVA hydro generator, after 50 years in service. The main purpose of this work is to characterize the stator mainwall insulation by PD testing with the emphasis on the dependencies on the test voltage frequency and temperature. The tested epoxy-mica based stator bars were taken from the high voltage side of the winding. Non-energized (unused) back-up bars were also tested to study the effect of aging on the PD characteristics and to set as a point of reference. The PD characterization was conducted at different frequencies (0.1, 1, and 50 Hz) and temperatures (30, 70, and 130 °C) at 8.9 kV (1.2 U_0). The observed frequency and temperature dependencies were discussed using theoretical findings regarding the mechanisms of void degradation and surface conductivity. Also, classification using supervised machine learning was briefly applied to discover patterns in the data as a function of frequency and temperature.**

I. Introduction

Intermittent power generation causes stator winding insulation of hydro generators to experience damaging and frequent service failures, resulting in long downtimes, costly repairs, thus, significant economic losses [1]. The evergrowing intermittent operation has raised concerns for the condition of the stator winding insulation of the Norwegian hydro generators that were designed for mostly continuous operation 50 years back [2]. Reliable and accurate condition monitoring of stator winding insulation has been widely performed using both off-line and on-line partial discharge (PD) measurements [2].

The use of very-low-frequency (VLF) high voltage (HV) sources, operating at 0.1 Hz and below, have recently been considered for the condition assessment of hydro generators [2], [3]. Their relatively small size and low cost compared to power frequency resonant sources have rendered VLF sources attractive alternatives for the PD testing of installed generators [2]. Although several test procedures are available [4], [5], little is known about the correlation between the PD features obtained at VLF and those at 50/60 Hz [6], [7].

Persistent PD activity may cause PD-induced aging (permanent changes) in the PD properties that may alter the voltage frequency dependency of PD activity. Recently, scholars have examined the effects of frequency on the PD characteristics. Nair et al. [8] performed frequency-dependent PD measurements on single stator coils with various artificial defects and concluded that measured frequency-dependent PD activity could be qualitatively explained with charge decay within the voids. Gulski et al. [9] reported that charge magnitudes and inception voltages of four different large motors were comparable at 50 Hz and 230 Hz damped AC. In [10], a comparative study between VLF off-line and on-line PD monitoring measurements on a 95-MVA-hydro generator was carried out. In a follow-up study [11], inception voltage and charge magnitude were reported to be comparable at 0.1 Hz and 50 Hz. Still, the literature on the VLF PD measurements for stator insulation is limited.

Generally, the machine insulation diagnosis by PD measurements is performed periodically; however, the surface temperature of stator bars during PD measurement may vary based on the recent operation mode, which may affect the PD characteristics [12]. For instance, the stator temperature is elevated to operating/service temperature during on-line measurements while it can be notably lower at off-line measurements. Thereby, it is also vital to know the surface temperature of stator bars to consider the effect of temperature on the PD diagnostics. Nonetheless, far too little attention has been paid to the effect of temperature.

This paper seeks to obtain data that help address these research gaps by performing PD characterization of the stator bars in the laboratory with a focus on the dependencies on the test voltage frequency and temperature.

II. Laboratory PD measurements

Initial PD measurements were performed on the extracted stator bars that had no apparent damage to the outer corona protection. The stator windings have Roebel transposed conductors and epoxy impregnated mica tape (Micadur) mainwall insulation with temperature class F (155 °C) [2], [11]. After the PD screening of all 163 stator bars, the stator bars were categorized into four main groups: bars taken close to the HV terminal (with low or high PD levels) and those taken close to the neutral terminal (with low or high PD levels). In this work, two bars with high PD activity taken from the HV terminal (U49 and U50) and one bar with low PD taken from the HV terminal were selected (U23). In addition, two non-energized (unused) back-up bars were used as a benchmark for comparison (R26 and R28). The original name tags of the bars given in the parentheses will be referred to in the figures and discussion to represent the chosen groups.

Before the experiments, the end-windings were removed as layers of asbestos were included in the end-winding design. Then, the semiconductive coating was removed from the service-aged stator bars, and field stress grading paint (CoronaShield P8001) was applied by following the manufacturer's instruction, as can be seen in Fig. 1. We presented in [2], [11] that both the phase-resolved PD (PRPD) patterns and PD levels

This is the accepted versjon of an article published in 2020 IEEE Conference on Electrical Insulation and Dielectric Phenomena (CEIDP)
https://doi.org/10.1109/CEIDP49254.2020.9437438

were similar after the application of the new stress grading. Interested readers can refer to [11] for more information on the initial measurements.

Fig. 1: Laboratory setup for the PD tests, including the heating chamber, to control the temperature.

A high voltage amplifier fed by a signal generator was used to energize the stator bars, and PDs were measured using a 2-nF coupling capacitor and commercial PD monitoring system (Omicron MPD), as illustrated in Fig. 2. Measurements were performed according to IEC 60270 [4] and with a pulse spectrum integrated ranging 40–840 kHz. The PD characteristics of the bars were investigated as a function of test voltage frequency and ambient temperature using statistical analysis based on basic discharge parameters, such as the 99 percentile maximum discharge magnitude, the number of discharges per cycle and second (repetition rate), and the phase-resolved PD pattern. High voltage AC with frequencies 0.1, 1, and 50 Hz were applied to the conductor, at a voltage level of 8.9 kV (1.2 U_0[1]) at 30 (ambient), 70 (service), and 130 °C (emergency). Metallic grounded electrodes simulating the stator slot were attached to the long main-wall section of the bars (Fig. 1). Before each experiment, each stator bar was PD preconditioned at 7.5 kV (U_0, 50 Hz) for 16 hours at the chosen temperature. The bars were placed in a temperature chamber in the experiments to control the temperature, as shown in Fig. 1. In the experiments, each stator bar was energized for 15 minutes at each frequency and temperature while PRPD patterns were accumulated. The PRPD data at each voltage frequency was post-processed using 90 cycles (periods), meaning that data for 15 min at 0.1 Hz, 1.5 min at 1 Hz, and 1.8 s at 50 Hz.

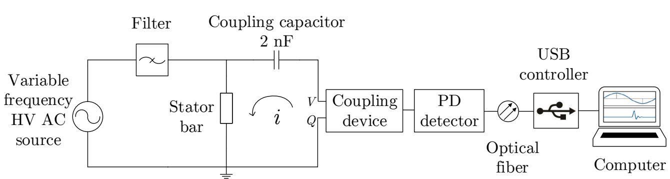

Fig. 2: Electrical circuit of PD measurement setup.

III. Results and Discussion

Figs. 3–4 present PRPD plots measured at 0.1, 1, and 50 Hz and 30, 70, and 130 °C for bars U50 (service-aged) and R28 (unused back-up bar for reference) with its original end-windings, respectively. As referred in Section II, 90 cycles of PRPD data at each frequency was recorded. The patterns in both the bars indicated symmetric discharge distribution with nearly equal in magnitude in both voltage half-cycles, suggesting cavity discharges due to internal delamination in the main-

[1]IEC 60034-27 mandates a maximum test voltage of $\sqrt{3}\,U_0$ [5].

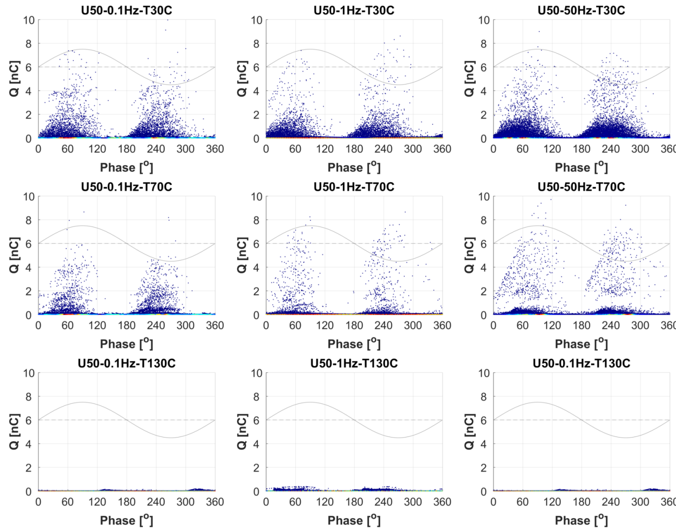

Fig. 3: PRPDA plots for U50 at 1.2 U_0.

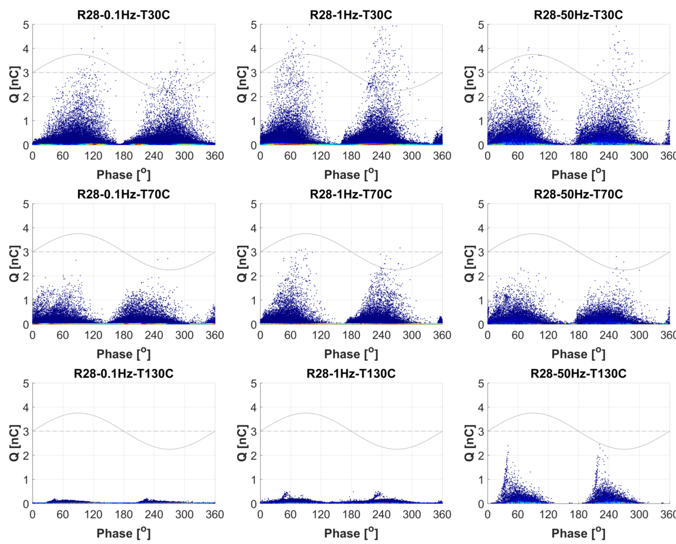

Fig. 4: PRPDA plots for R28 at 1.2 U_0.

wall insulation [8], [13]. Besides, larger PD magnitudes with an increased number of PDs were observed towards higher frequencies at all temperatures. Toward higher temperatures, both the PD magnitude and the number of PDs dropped.

To incorporate the results of all the tested stator bars, we used box plots to represent the 99 percentile maximum charge magnitude (Q_{max}), the discharge repetition rate per cycle (PDs/cycle), and the total number of discharges per second (PDs/s) as a function of frequency and temperature, as demonstrated in Figs. 5–6. Fig. 5 depicts the Q_{max} of each stator bar using box plots.[2] As seen in the figure, unused bars (R26 and R28) reached to larger Q_{max} than did the aged bars. Especially, U23 had the lowest value with the smallest confidence interval. These observations accord well with the reported trend in PD magnitudes over time for stator windings

[2]On each box, the central mark indicates the median, and the bottom and top edges of the box indicate the 25^{th} and 75^{th} percentiles, respectively. The whiskers extend to the most extreme data points not considered outliers, and the outliers are plotted individually using the + symbol.

This is the accepted versjon of an article published in 2020 IEEE Conference on Electrical Insulation and Dielectric Phenomena (CEIDP)
https://doi.org/10.1109/CEIDP49254.2020.9437438

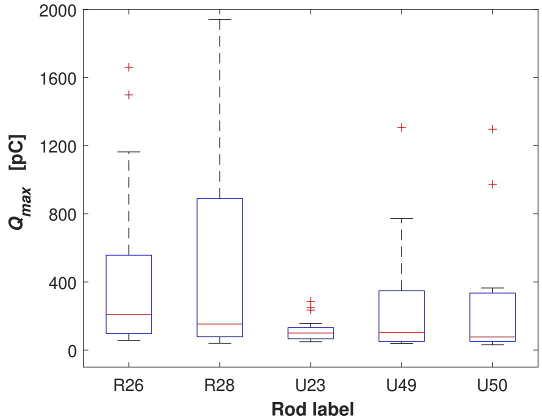

Fig. 5: Q_{max} obtained in different stator bars.

in [14] that PD magnitude was lower in used bars compared to new windings.

PDs produce acidic by-products when in contact with the surrounding gas and dielectric surface, resulting in a significantly increased surface conductivity [15], [16]. In time, aging caused by persistent PD activity is likely to erode the surface of the void and can result in further increased surface conductivity [15]. Increased surface conductivity accelerates the decay of residual charges due to conduction; thus, the decay time is reduced by several orders of magnitude. Consequently, voids can partially or entirely be short-circuited, resulting in reduced discharge activity and magnitude [8]. Increased conductivity in aged bars could then be the reason why the unused back-up bars had relatively high Q_{max}.

For all the bars represented in Fig. 6(a), there was an increase in Q_{max} at higher frequencies, which is consistent with the reported studies that claimed that PD magnitude was lower at lower excitation frequencies due to significant charge decay [8]. The repetition rate (PDs per cycle) was significantly higher at 0.1 Hz, while the total number of discharges per second (PDs/s) was the highest at 50 Hz (90 cycles at each frequency)—see Figs. 6(b)–6(c). Nair et al. [8] observed identical trends such that the number of discharges per cycle of both polarities increased with the reduction in the frequency. An account of this behavior might be that more surface charges are likely to be present at the void surface at higher frequencies due to slow charge decay, thus enhancing the surface-emission of electrons [17]. Furthermore, Edin [18] concluded in his dissertation that at frequencies below 1 Hz, the discharge activity decreased with decreasing frequency due to the increasing influence of the surface conductivity of the cavities and the delaminations. He showed that increased surface conductivity yielded a higher inception voltage of surface streamers by altering the electrical field and thus caused a reduction of the tangential field at decreasing frequencies, which led to the ceasing of discharges at low frequencies [18].

In assessing the frequency and temperature dependence of discharge magnitude and repetition rate, it is important to bear in mind that voids and possible delaminations of various sizes in the stator bars may lead to different PD responses to the applied test voltage. As can be seen in Fig. 7, in the case of U23, there was almost no PD at the polarity reversal at both 0.1 Hz and 50 Hz, suggesting that deposited surface discharges decayed rapidly. In the case of U50, on the other hand, there were PDs at the polarity reversal at both frequencies

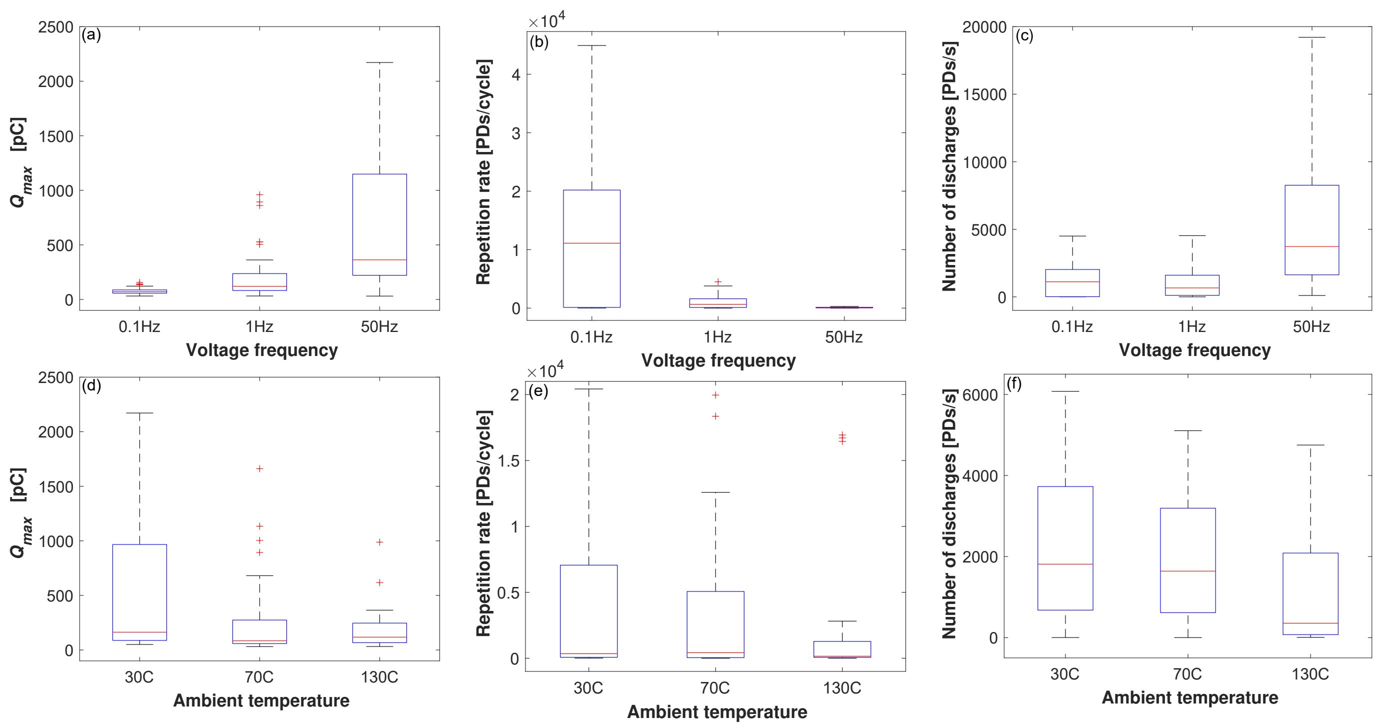

Fig. 6: Box plot representing the results of Q_{max}, repetition rate, and the total number of discharges at different frequencies (0.1, 1, and 50 Hz) and temperatures (30, 70, and 130 °C) at 8.9 kV (1.2 $\boldsymbol{U_0}$).

This is the accepted versjon of an article published in 2020 IEEE Conference on Electrical Insulation and Dielectric Phenomena (CEIDP)
https://doi.org/10.1109/CEIDP49254.2020.9437438

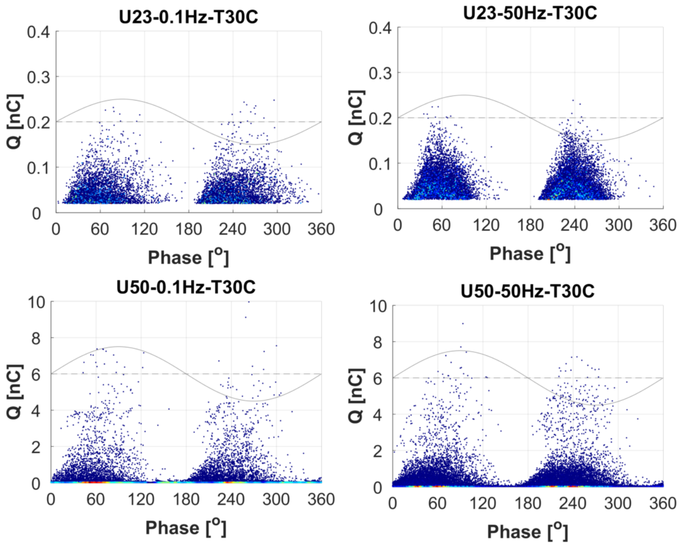

Fig. 7: PRPDA of U23 and U50 at 0.1 and 50 Hz at 30 °C and 1.2 U_0.

with fewer PDs at 0.1 Hz. These observations imply that the deposited surface charges have more time to decay further at 0.1 Hz, and thus, do not contribute to the local electric field at polarity reversal compared to the case at 50 Hz, which is in good agreement with the above-mentioned reported results.

Temperature dependency of the PD features is exhibited in Figs. 6(d)–6(f). As displayed in Fig. 6(d), Q_{max} decreased when the temperature was increased. The variances of both the repetition rate (PDs/cycle) and the number of discharges per second (PDs/s) were somewhat higher at 30 °C compared to that at 130 °C while the median values were similar [see Figs. 6(e)–6(f)]. Although these findings are in line with what is usually observed in insulation materials where the conductivity increases with temperature, they do not fully agree with the findings of Aakre et al. [16], where they tested lab-made, resin-rich samples with small and large voids. They concluded that PD by-products diffuse faster than they are produced at elevated temperatures, reducing the acidity, and thereby the surface conductivity [16]. The results here, hence, need to be interpreted with caution because the mechanisms of conductivity do not follow a simple theory, but rather a complex process in which the conductive species are created that decay in time and decay faster at higher temperatures [16].

Aakre et al. [16], [19] claimed that the stator bars with small voids/delaminations have a different correlation between void conductivity and temperature than the objects with larger voids, and by-products in smaller voids do not decay as fast as those in larger voids. Therefore, the void volume seems to be a key factor for by-product relaxation. Moreover, Nair et al. [12] found that there was an increase in the magnitude of slot discharges (occurring at a large surface area) at higher surface temperatures. In light of these findings, Q_{max} values in Fig. 6(d) imply that, at higher temperatures, PD by-products probably deposited at the void surfaces and increased the conductivity because the sizes of the internal voids/delaminations were likely to be relatively small, having led to a slower decay rate. For a better evaluation, Aakre et al. [16], [19] proposed that temperature dependency of the frequency-dependent dielectric response and DC conductivity of the insulation need to be determined and taken into account when modeling the correlation between the PD characteristics of stator mainwall insulation and temperature because they found that the material conductivity and frequency-dependent dielectric response also vary with temperature. Therefore, further research is needed to determine the dielectric response, DC conductivity, and their temperature dependence to be able to discuss the effect of temperature thoroughly.

Lastly, we plotted Q_{max} data versus the repetition rate, as shown in Fig. 8, to explore natural patterns (if any) in the data as a function of frequency and temperature. As seen in Fig. 8(a), distinctive patterns were observed at different frequencies such that in the case of 0.1 Hz, the data lies horizontally with low Q_{max} while in the case of 50 Hz, data points are spread almost vertically, reaching very high Q_{max} values. However, when the same data was grouped versus temperature, as shown in Fig. 8(b), finding any pattern was not straightforward. To that end, by implementing supervised machine learning (ML) using the Classification Learner App on MATLAB, a support vector machine (SVM) model was trained using a part of the data (observations). Then, the model was tested using the rest of the data (observations not used in the training) to look for patterns based on the already known categorical variables of frequency or temperature for each observation (supervised). The used PD features to train the model incorporated not only the PD characteristics shown in this work but also other statistical quantities (average discharge current, discharge power, etc.) calculated based on the guidelines in IEC 60270 [4].

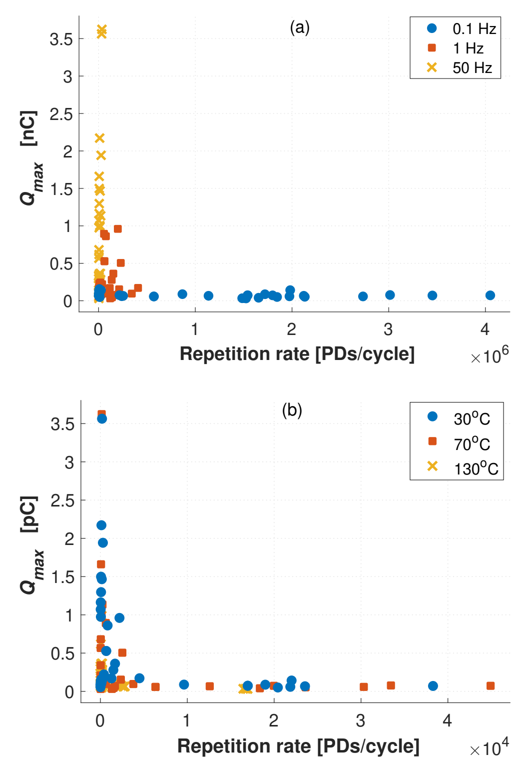

Fig. 8: Q_{max} vs. repetition rate: (a) in frequency. (b) in temperature.

This is the accepted versjon of an article published in 2020 IEEE Conference on Electrical Insulation and Dielectric Phenomena (CEIDP)
https://doi.org/10.1109/CEIDP49254.2020.9437438

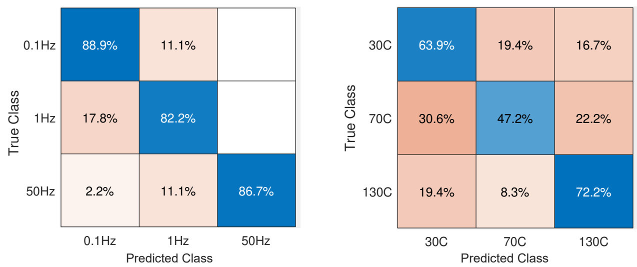

(a) Classification vs. frequency. (b) Classification vs. temperature.

Fig. 9: Confusion matrix generated by MATLAB's Classification Learner using the Q_{max} vs. frequency data.

Fig. 9(a) displays the confusion matrix for the classification problem: the model was able to predict the data points (observations) that belong to different frequencies with an average accuracy of 85.9%. There were few falsely predicted data points, probably at the boundaries of the segregated groups. The model did not confuse any data points at 0.1 Hz and 1 Hz with those at 50 Hz. On the other hand, it performed worse in the case of the classification for temperature dependency with an average accuracy of 61.1% [see Fig. 9(b)]. It is not surprising when the lack of clear patterns observed in Fig. 8(b) is considered. These findings further support the need for including the dielectric response and DC conductivity in the model to elucidate the correlation between the PD characteristics and temperature.

IV. Conclusion

The main goal of the current study was to characterize stator mainwall insulation by PD testing with the emphasis on the dependencies on the test voltage frequency and temperature. Results indicated that the PRPD pattern of internal delamination discharge was symmetric at all test frequencies (0.1, 1, and 50 Hz) and temperatures (30, 70, and 130 °C).

It was shown that increased conductivity in aged bars was likely to be the culprit of lower discharge magnitudes measured in the case of the unused back-up bars. Considering the test results of all the bars, we observed that discharge magnitude and the number of discharges increased at higher frequencies due to a possible charge decay at lower excitation frequencies. Thus, the relevance of the voltage frequency was clearly supported by the current findings.

On the other hand, the discharge magnitude and the number of discharges were found to be decreasing at higher temperatures. The results obtained at elevated temperatures were consistent with what is usually observed in insulation materials where the conductivity increases with temperature. However, opposite trends at higher temperatures were also reported in several studies. Hence, further research is required to explain the correlation between PD characteristics and temperature. Studies including the temperature dependency of the dielectric response (in a broad frequency spectra) and DC conductivity of the insulation are likely to provide more insight.

Finally, though the use of machine learning was not intended to model the PD characteristics as a function of frequency and temperature, the model was able to detect distinguishable patterns in the data, especially between VLF and 50 Hz, with very high accuracy. A future study investigating the patterns at different temperatures, including the data of the additional research suggested above, is worthy of attention.

References

[1] Working Group A1.10, "Survey of Hydrogenerator Failures," 2009. [Online]. Available: https://e-cigre.org/publication/392-survey-of-hydrogenerator-failures
[2] E. Eberg, G. Berg, S. Hvidsten, E. Kantar, and L. Lone, "Partial discharge characterization of stator windings taken from a hydro generator after 50 years of service," in *CIGRE Session 48*, 2020, pp. A1–205.
[3] T. G. Aakre, E. Ildstad, and S. Hvidsten, "Condition assessment of hydrogenerator stator bar insulation using partial discharge measurements," in *IEEE Electr. Insul. Conf. (EIC)*. IEEE, 2018, pp. 357–360.
[4] International Electrotechnical Commission, "IEC 60270:2000 High-voltage test techniques - Partial discharge measurements," 2000.
[5] International Electrotechnical Commission, "IEC 60034-27-1:2017 Rotating Electrical Machines–Part 27-1: Off-line Partial Discharges Measurements on the Winding Insulation," 2017.
[6] C. Forssén and H. Edin, "Partial discharges in a cavity at variable applied frequency part 1: measurements," *IEEE Trans. Dielectr. Electr. Insul.*, vol. 15, no. 6, pp. 1601–1609, 2008.
[7] A. Cavallini and G. C. Montanari, "Effect of supply voltage frequency on testing of insulation system," *IEEE Trans. Dielectr. Electr. Insul.*, vol. 13, no. 1, pp. 111–121, 2006.
[8] R. P. Nair and S. B. Vishwanath, "Analysis of partial discharge sources in stator insulation system using variable excitation frequency," *IET Sci. Meas. Tech.*, vol. 13, no. 6, pp. 922–930, 2019.
[9] E. Gulski, S. Meijer, H. Van Breen, P. Seitz, F. De Vries, and F. Petzold, "Partial discharge diagnosis of stator insulation using damped ac voltages," in *IEEE Int. Symp. Electr. Insul.* IEEE, 2006, pp. 6–9.
[10] E. Eberg, T. G. Aakre, G. Berg, and S. Hvidsten, "Comparison of offline vlf pd measurements and online pd measurements on a 50-year-old hydrogenerator stator in norway," in *IEEE Electr. Insul. Conf. (EIC)*. IEEE, 2018, pp. 542–546.
[11] G. Berg, E. Eberg, and S. Hvidsten, "Partial discharge characterisation of stator windings taken from a 50-year-old norwegian hydrogenerator," in *IEEE Electr. Insul. Conf. (EIC)*. IEEE, 2019, pp. 168–171.
[12] R. P. Nair, B. V. Sumangala, B. N. Rao, and Thirumurthy, "Effect of temperature on slot discharge pattern measured in stator coils at variable frequency sinusoidal voltage excitation," in *12th Int. Conf. Prop. App. Dielectr. Mater. (ICPADM)*, 2018, pp. 257–261.
[13] C. Hudon and M. Belec, "Partial discharge signal interpretation for generator diagnostics," *IEEE Trans. Dielectr. Electr. Insul.*, vol. 12, no. 2, pp. 297–319, 2005.
[14] G. C. Stone, "A perspective on online partial discharge monitoring for assessment of the condition of rotating machine stator winding insulation," *IEEE Electr. Insul. Mag.*, vol. 28, no. 5, pp. 8–13, 2012.
[15] C. Hudon, R. Bartnikas, and M. R. Wertheimer, "Effect of physico-chemical degradation of epoxy resin on partial discharge behavior," *IEEE Trans. Dielectr. Electr. Insul.*, vol. 2, no. 6, pp. 1083–1094, 1995.
[16] T. G. Aakre, E. Ildstad, and S. Hvidsten, "Partial discharge inception voltage of voids enclosed in epoxy/mica versus voltage frequency and temperature," *IEEE Trans. Dielectr. Electr. Insul.*, vol. 27, no. 1, pp. 214–221, 2020.
[17] C. Forssen and H. Edin, "Partial discharges in a cavity at variable applied frequency part 2: measurements and modeling," *IEEE Trans. Dielectr. Electr. Insul.*, vol. 15, no. 6, pp. 1610–1616, 2008.
[18] H. Edin, "Partial discharges studied with variable frequency of the applied voltage," Ph.D. dissertation, KTH, 2001.
[19] T. G. Aakre, "Partial discharges in voids at variable voltage frequency and temperature diagnostic testing of stator mainwall insulation," Ph.D. dissertation, NTNU, 2020.

This is the accepted versjon of an article published in 2020 IEEE Conference on Electrical Insulation and Dielectric Phenomena (CEIDP)
https://doi.org/10.1109/CEIDP49254.2020.9437438